remote sensing

MDPI

Article

Developing an Atlas of Harmful Algal Blooms in the Red Sea: Linkages to Local Aquaculture

Elamurugu Alias Gokul [1], Dionysios E. Raitsos [2], John A. Gittings [1] and Ibrahim Hoteit [1,*]

[1] Earth Science and Engineering (ErSE), King Abdullah University of Science and Technology (KAUST), Thuwal 23955, Kingdom of Saudi Arabia. rajadurai.elamurugu@kaust.edu.sa (E.A.G.), john.gittings@kaust.edu.sa (J.A.G.)

[2] Department of Biology, National and Kapodistrian University of Athens (NKUA), Athens 15784, Greece. draitsos@biol.uoa.gr (D.E.R)

* Correspondence: Ibrahim.hoteit@kaust.edu.sa

Received: 11 September 2020; Accepted: 2 November 2020; Published: date

1. **Supplementary Materials**

1.1. Remotely Sensing harmful algal blooms (HABs) , and the Wind Patterns in the Red Sea

In this section, we present satellite-derived HAB maps, alongside wind patterns over the regions where in situ sampling was conducted in the Red Sea, during different periods from 2003 to 2017. We further implemented the remote sensing algorithm of Gokul et al. [1] to identify the phytoplankton species that were responsible for the HAB outbreaks, based on their unique R_{rs} spectral characteristics. We then validate these remotely sensed HABs with concurrent in situ sampling locations from different HAB sampling campaigns conducted in the Red Sea over the last two decades (Table S1). Firstly, we produced HAB maps by applying the remote sensing algorithm of Gokul et al. [1], which is based on the satellite derived R_{rs} spectra, in order to detect and map the spatial distribution of HAB events in the Red Sea. Secondly, we utilized satellite derived ocean surface vector wind products in order to examine the wind speed and direction during the HAB event. We note that the gridded ocean surface vector wind products were obtained from the 10-year archive of QuikSCAT from 1999 to 2009, and the 13-year archive of Advanced Scatterometer (ASCAT) from 2007 to 2020.

We first detected the presence of dinoflagellates *Ostreopsis* sp. and cyanobacteria *Trichodesmium erythraeum* during summer 2013 and 2004 along the coastal areas of Thuwal (NCRS) and Jeddah (NCRS), respectively. The model was found to match markedly well with the concurrent in situ HAB sampling locations that were reported by previous studies [2,3] (HAB map of Thuwal and Jeddah region in Figure S1). The prevailing north-westerly wind patterns were clearly observed over the region of Thuwal and Jeddah during summer 2013 and 2004, respectively (wind speed map of Thuwal and Jeddah in Figure S1). In summer 2010, we detected the presence of raphidophytes *Heterosigma akashiwo* blooms in the coastal waters of Al-Lith, which was found to be in good agreement with the concurrent in situ HAB sampling location of Mohamed and Al-Shehri [4] (Figure S1). Similar to NCRS, the north-westerly wind patterns were clearly observed over the Al-Lith region during summer 2010 (wind speed map of Al-Lith region in Figure S1).We detected the presence of dinoflagellates *Noctiluca scintillans/miliaris* in the region of Doga during 2004 and mapped their spatial distribution along the east coast of the SCRS (Figure S1). The *N. scintillans/miliaris* blooms detected by the remote sensing model were found to concur with previous studies [5] conducted along the east coastal waters of SCRS region during summer 2004. The prevailing north-westerly wind patterns were evident in the east coast of SCRS during summer 2004 and 2011 (Figure S1).

Table S1. Summary of the harmful algal bloom (HAB) species reported by the various studies in the Red Sea waters.

Name of the Harmful Algal Bloom	Sampling Locations	Season of HAB Abundance	References
Ostreopsis sp.	Coasts of Thuwal, (NCRS) (*22° 19.630′ N, 38° 51.440′ E*)	Summer (2013)	[2]
Trichodesmium erythraeum	Coasts of Jeddah (NCRS) (21°40′N, 39°10′E)	Summer (2004)	[3]
Heterosigma akashiwo	Coasts of Al-Lith (SCRS) (*19°59′05″ N, 40°23′20″ E*)	Summer (2010)	[4]
Noctiluca scintillans/miliaris	Coasts of Doga (SCRS) (19°65′N,42°18′E)	Summer (2004)	[5]
Noctiluca scintillans/miliaris	Coast of Al Hodeida City (SRS) (*14°22′26″ N, 42°56′27″ E*)	Winter (2009)	[6]
Pyrodinium bahamense and Trichodesmium erythraeum	Coast of Al Hodeida City (SRS) (*14° 47′ 07″ N, 42° 56′ 46.31″ E*)	Winter (2012)	[7]

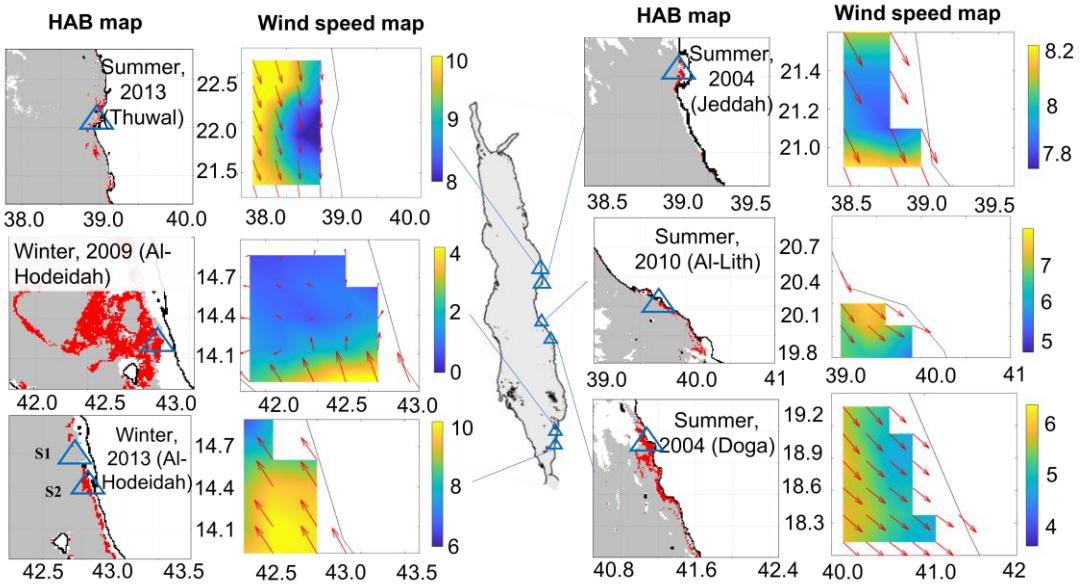

Figure S1. Remotely sensed HAB events and the wind speed (m/s) patterns over the regions where the in situ sampling was conducted in the Red Sea during the different periods from 2003 to 2017. The blue triangles indicate the in situ sampling location of the HAB events.

During winter 2009, we identified *N. scintillans/miliaris* blooms along the coastal water of Yemen and mapped their spatial distribution over the open waters of the SRS. The remotely sensed *N. scintillans/miliaris* blooms coincided with the in situ sampling location of the HAB event reported by Alkershi and Menon [6] during winter 2009 along the coastal waters of Al-Hodeidah (Figure S1). In addition, we detected the presence of *Pyrodinium bahamense* along the coastal waters of Al-Hodeidah during the winter of 2013. The model detection matches markedly well with the in situ sampling location (Figure S1) that was reported by Alkawari et al., [7]. In addition, Alkawari et al., [7] reported a cyanobacteria *T. erythraeum* blooms, that were spatially less dense, along with the dinoflagellates *P. bahamense* in the coastal waters of Yemen during winter 2013. However, the remote sensing algorithm of Gokul et al. [1] was limited at detecting the HABs that are spatially less dense, and/or composed of mixed assemblages of phytoplankton (especially cyanobacteria with dinoflagellates) (see Station "S1" in the HAB map of Al-Hodeidah (winter, 2013) of Figure S1). Unlike the NCRS and SCRS, the prevailing south-easterly wind patterns were clearly evident in the satellite-derived wind speed map over SRS (Figure S1) that promote the northward advection of nutrient-rich surface waters into the Red Sea from the Gulf of Aden [8–11] and could disseminate the aforementioned HAB species over the SRS region during winter 2009 and 2013 [6,7,12].

1.2. Time Series Analysis of Satellite-Derived Chl-a Concentrations

In order to further explore between HABs and *Chl-a* concentrations (a proxy for nutrient concentration), in the Red Sea, we presented a time series analysis of satellite derived *Chl-a* concentrations, over the regions where the in situ sampling was conducted in the Red Sea during the different periods from 2003 to 2017 (Figure S2). During 2013 and 2004, elevated *Chl-a* concentrations were observed during May and June in the coastal waters of Thuwal and Jeddah, respectively. Similarly, the time series analysis in the coastal waters of Al-Lith, and Doga revealed that maximum *Chl-a* concentrations were observed during the summer season (between May–August). In contrast, we observed maximum *Chl-a* concentrations over the winter season (February–March) during 2009 and 2013 in the coastal waters of Al-Hodeidah (SRS). It is worthwhile to note that remotely sensed *Chl-a* observations were limited over the summer season in Al-Hodeidah due to the adverse atmospheric conditions (haze and cloud) in the SRS [1,13–15].

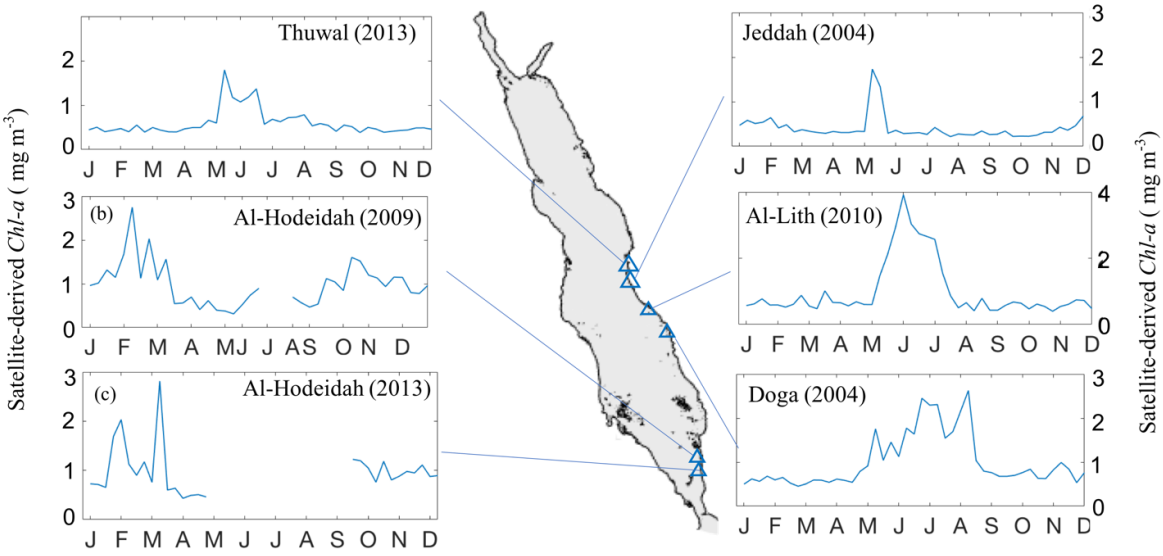

Figure S2. Time series analysis of satellite derived *Chl-a* over the regions where the in situ sampling was conducted in the Red Sea during the different periods from 2003 to 2017. The blue triangles indicate the in situ sampling location of the HAB events. The Chl-a dataset was acquired from version 4.1 of the ESA OC-CCI product.

1.3. Interactions of HABs with Aquaculture: Case Studies

We highlighted the potential interactions between HABs and an aquaculture facility through the case studies from the coastal waters of Al-Lith, Saudi Arabia. To emphasize this, we produced two daily, cloud-free images of R_{rs} and *Chl-a* concentration at a 300 m spatial resolution, for 6th May 2004 and 27th May 2010, for detecting the presence/absence of HABs and mapping their spatial distribution in the vicinity of Al-Lith's aquaculture facility (Figure S3 and S4). Firstly, we investigated the *Chl-a* concentrations during the HAB event in the proximity of Al-Lith's aquaculture facility using satellite derived *Chl-a* concentrations. Secondly, we produced the HAB maps by applying the remote sensing algorithm of Gokul et al. [1], which is based on the satellite derived R_{rs} spectra, in order to detect the presence/absence and map the spatial distribution of HAB events in the vicinity of Al-Lith's aquaculture facility. Following this, we utilized satellite derived ocean surface vector wind products in order to show the wind speed and direction during the HAB event.

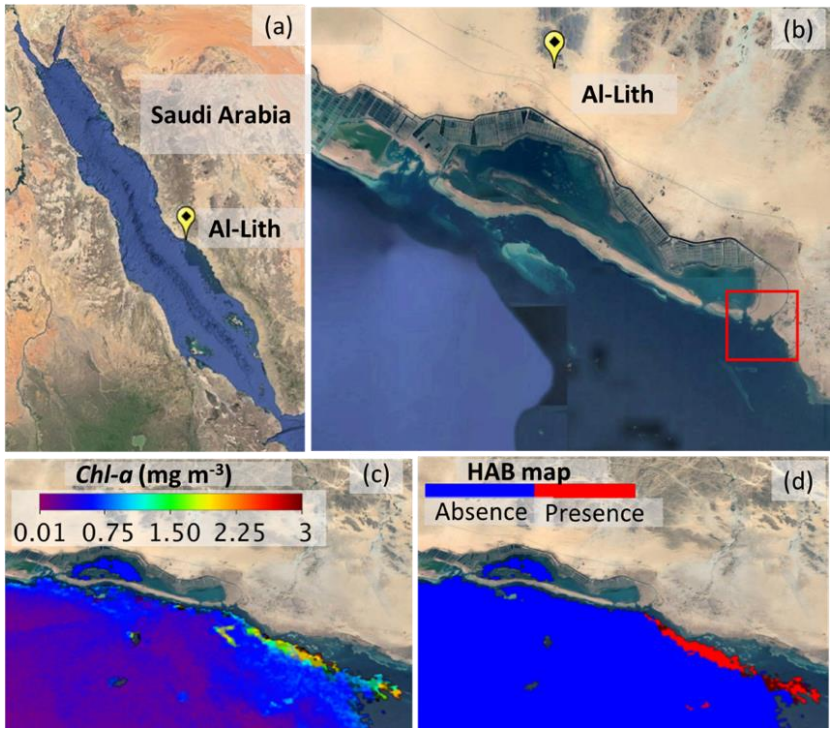

Figure S3. Remotely sensing HAB event in the Al-lith aquaculture facility. **(a)** and **(b)** Maps showing the location of the aquaculture facility in Al-Lith, Saudi Arabia (yellow pin), in the central Red Sea (red box indicates the location of aquaculture outfall (20.1556°N; 40.2499°E)). **(c)** Satellite-derived *Chl-a* map. **(d)** MERIS-derived HAB map highlighting the presence and absence of HABs in the vicinity of Al-Lith's aquaculture facility on 6th May 2004.

We investigated the satellite-derived *Chl-a* concentrations and found that high *Chl-a* concentrations (> 1 mg m^{-3}) were observed in the proximity of Al-Lith's aquaculture facility (Saudi Arabia) (Figures S3c and S4a). We then implemented the remote sensing algorithm for generating the HAB map in the case study area. As shown in Figure S3d and S4b, the HAB pattern as depicted by the presence/absence HAB map coincides spatially with high *Chl-a* values (> 1 mg m^{-3}) in the proximity of Al-Lith's aquaculture outfall. To support this observation, previous studies using satellite and/or in situ observations have demonstrated that *Chl-a* values exceeding the minimum value of ~1 mg m^{-3} constituted a HAB event along the Saudi Arabian Red Sea coast during the summer season [1,3,4]. As evident in Figure S4c, the presence of a remotely sensed HAB event was found to coincide with in situ sampling of raphidophytes (*H. akashiwo)* that were collected in the vicinity of Al-Lith's aquaculture facility on 27th May 2010 [4]. The prevailing north-westerly wind patterns were observed over the region of Al-Lith during 27th May 2010 and had an average speed of 5.5 m/s (Figure S4d).

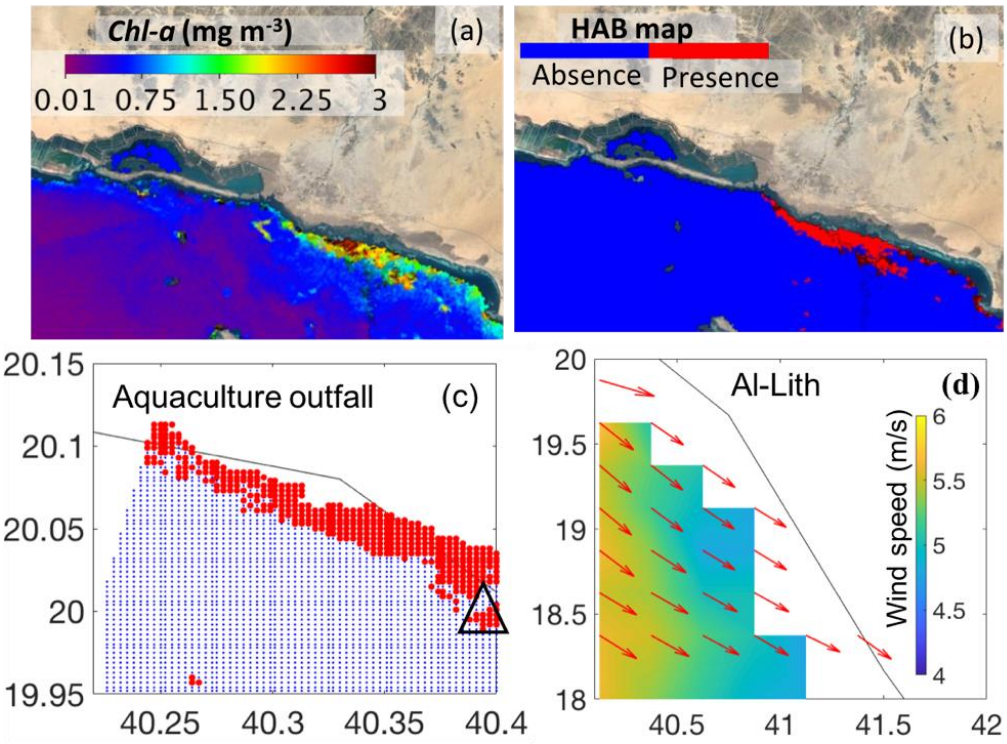

Figure S4. Remotely sensing HAB event in the Al-lith aquaculture facility) (**a**) Satellite-derived *Chl-a* map. (**b**) and (**c**) MERIS-derived HAB map highlighting the presence and absence of HABs in the vicinity of Al-Lith's aquaculture facility on 27th May 2010. (In (**c**) red and blue dots indicate presence and absence of remotely sensed HAB event, respectively; Black triangle indicates *in situ* sampling location of HAB event) (**d**) Satellite-derived wind speed map during 27th May 2010.

References

1. Gokul, E.A.; Raitsos, D.E.; Gittings, J.A.; Alkawri, A.; Hoteit, I. Remotely sensing harmful algal blooms in the Red Sea. *PloS one*. **2019**,14, e0215463.
2. Catania, D.; Richlen, M.L.; Mak, Y.L.; Morton, S.L.; Laban, E.H.; Xu, Y.; Anderson, D.M.; Chan, L.L.; Berumen, M.L. The prevalence of benthic dinoflagellates associated with ciguatera fish poisoning in the central Red Sea. *Harmful algae*. **2017**, 68, 206– 216.
3. Touliabah, H.E.; Abu El-Kheir, W.S.; Kuchari, M.G. Phytoplankton composition at Jeddah coast-Red Sea, Saudi Arabia in relation to some ecological factors. *J. King Abdulaziz Univ. Science*. **2010,** 148, 1-34.
4. Mohamed, Z.A.; Al-Shehri, A.M. The link between shrimp farm runoff and blooms of toxic Heterosigma akashiwo in Red Sea coastal waters. *Oceanologia*. **2012**, 54, 287–309.
5. Mohamed, Z.A.; Mesaad, I. First report on Noctiluca scintillans blooms in the Red Sea off the coasts of Saudi Arabia: consequences of eutrophication. *Oceanologia*. **2007**, 49, 337-351.
6. Alkershi, A.; Menon, N. Phytoplankton in polluted waters of the Red Sea coast of Yemen. *J. Mar. Biol. Ass. India*. **2011**, 53, 161–166.
7. Alkawri, A.; Abker, M.; Qutaei, E.; Alhag, M.; Qutaei, N.; Mahdy, S. The first recorded bloom of Pyrodinium bahamense var bahamense plate in Yemeni coastal waters off Red Sea, near Al Hodeida City. Turk. J. Fish. Aquat. Sci. 2016b, 16, 275–282.
8. Murray, S.P.; Johns, W. Direct observations of seasonal exchange through the Bab el Mandab Strait. Oceanogr. Lit. Rev. 1998, 3, 438.
9. Johns, W.E.; Sofianos, S.S. Atmospherically-forced exchange through the Bab el Mandeb. The 2nd Meeting on the Physical Oceanography of Sea Straits. 2002 ,(pp. 135-138).

10. Yao, F.; Hoteit, I.; Pratt, L.J.; Bower, A.S.; Köhl, A.; Gopalakrishnan, G.; Rivas, D. Seasonal overturning circulation in the Red Sea: 2. Winter circulation. J. Geophys. Res. Oceans. 2014b, 119, 2263-2289.
11. Triantafyllou, G.; Yao, F.; Petihakis, G.; Tsiaras, K.P.; Raitsos, D.E.; Hoteit, I. Exploring the Red Sea seasonal ecosystem functioning using a three-dimensional biophysical model. J. Geophys. Res. Oceans. 2014, 119, 1791-1811.
12. Mohamed ZA. Potentially harmful microalgae and algal blooms in the Red Sea: Current knowledge and research needs. Marine environmental research. 2018 Sep 1;140:234-42.
13. Steinmetz, F.; Deschamps, P.Y.; Ramon, D. Atmospheric correction in presence of sun glint: application to MERIS. *Opt. Express*. **2011**, 19, 9783–9800.
14. Raitsos, D.E.; Yi, X.; Platt, T.; Racault, M.F.; Brewin, R.J.; Pradhan, Y.; Papadopoulos, V.P.; Sathyendranath S, Hoteit, I. Monsoon oscillations regulate fertility of the Red Sea. *Geophys. Res. Lett*. 2015, 42, 855–862.
15. Brewin, R.J.; Raitsos, D.E., Pradhan, Y.; Hoteit, I. Comparison of *Chl-a* in the Red Sea derived from MODIS- Aqua and in vivo fluorescence. *Remote Sensing of Environment*. **2013**, 136, 218–24.